J. Andersen (ed.), Reports on Astronomy, Vol. XXIVA, 115–139.

COMMISSION 16 : PHYSICAL STUDY OF PLANETS AND SATELLITES

(ETUDE PHYSIQUE DES PLANETES ET DES SATELLITES)

PRESIDENT: C. de Bergh
VICE-PRESIDENT: D.P. Cruikshank
SECRETARY: A. Coradini
ORGANIZING COMMITTEE: M.J.S. Belton, C. Blanco, G.J. Consolmagno, D. Gautier, M.Ya Marov, M.A. McGrath, K.S. Noll, T.C. Owen, V.G. Teifel & A. Woszczyk

1. INTRODUCTION

This report includes some of the major achievements in studies of planets and satellites that have been made during the past three years.

2. VENUS: GEOLOGY AND GEOPHYSICS

(Contributed by R. Stephen Saunders, and Martha S. Gilmore, Jet Propulsion Laboratory, Pasadena, USA)

Continuing analysis of craters on the surface of Venus has led to revised estimates for the average surface age. McKinnon et al. (1997) have revised the estimate of the surface age of Venus to a range of up to 800 Ma. Previous work that used crater statistics to date terrains scattered across the globe e.g., volcanics (Price et al. 1994; Namiki & Solomon 1994), tessera terrain (Ivanov & Basilevsky 1993; Gilmore et al. 1997) has been criticized because of the assumption that terrains of similar morphology occurred at distinct time intervals. This problem is the focus of a study by Hauck et al. (1998) who demonstrate that neither a random nor nonrandom crater distribution can be excluded to explain the observed population of craters.

The global contemporaneity of material units is probably the most debated topic in the Venus community. Mapping of a significant (~30%) portion of Venus by Basilevsky and Head, Ivanov and Head have identified units that have consistent stratigraphic positions throughout the map area. Basilevsky and Head have also found these plains are laterally contiguous over large portions of the surface, further supporting the idea that the plains represent a global geologic history, and that defined plains units occupy a specific stratigraphic position even when separated by large distances. This scheme has recently been called into question by Guest and Stofan (1999), who make observations of coronae and associated plains units that demonstrate that they occupy different stratigraphic levels at different areas of the planet, and that coronae evolve and erupt in a complicated way through time. They use such detailed observations to show that the general stratigraphic scheme of Basilevsky and Head does not always hold, everywhere. This debate illuminates the need to compare regional and local studies for an improved understanding of the extent and stratigraphic position of material units on the surface.

The definition of material units also continues to evolve. Perhaps the most famous plains unit is the plains with wrinkle ridges, which cover ~70% of the planet. While many workers, including Basilevsky and Head, treat the wrinkle ridges as a fundamental characteristic of these plains, other workers point out that the formation of wrinkle ridges is a tectonic process independent of plains formation, and perhaps related to local, rather

than global stress fields (e.g., McGill 1993). Much debate has also centered around the interpretation of extensional structures within tessera terrain as early tension fractures, supporting the formation of tessera over mantle upwellings (Hansen & Willis 1996 ; 1998; Ghent & Hansen 1999; Phillips & Hansen 1998) or as later stage graben supporting mantle downwellings (Gilmore et al. 1998; Bindschadler et al. 1992). Both models accommodate an early era of tessera formation, and more detailed mapping of tessera will be required to address questions about this most important terrain.

The average age of the surface and the mechanism of resurfacing (global or local) is critically dependent on the original observation by Schaber et al. (1992) that only ~4% of the craters are modified by volcanism. This is the primary supporting evidence that the resurfacing of Venus was global and occurred within a relatively short interval of time (100Ma scale; Collins et al. 1999). This observation has recently been brought into question by Herrick and Sharpton, who used high resolution digital terrain models to examine craters and found that dark floor craters were shallower than their bright floor counterparts. They interpret these data to mean that the numerous dark floor craters have been embayed by volcanic materials. While this evidence is compelling, the nature of such deposits, whether related to regional plains formation or impact-related, remains in question.

Work continues on geodynamic models for the history of Venus; the idea that Venus underwent a significant change from a more active planet to more passive, one-plate planet approximately 500 ma ago remains. This change has been attributed to a change from thin-skinned to more thick-skinned deformation due to the secular cooling of the planet through time (Solomotov and Moresi, 1996). The previous venusian era may have been one of plate-tectonics (Turcotte 1993; Turcotte et al. 1999), or vertical delamination events due to build up of buoyant depleted mantle (Parmentier and Hess 1992). Phillips and Hansen (1998) advocate a model where a plume formation during the thin crust era resulted in the formation of plateaus (tessera terrain), the same plumes result in large volcanic rises (Beta, Atla) during today's thick crust regime. An innovative idea has recently come from Bullock and Grinspoon (1999) whose models show that a hotter venusian atmosphere associated with an enhanced greenhouse due to gases associated with global volcanic resurfacing, show that the surface may have reached temperatures close to the brittle-ductile transition. Solomon et al. (1997) suggest that significant amounts of strain may have been recorded during this era. This may account for the general decrease in tectonically modified terrains with time in the stratigraphic history of Venus.

References

Basilevsky, A. T. & Head, J. W. 1995a, Earth, Moon and Planets, 66, 285-336

Basilevsky, A. T. & Head, J. W. 1995b, Planet. Space Sci., 43, 1523-1553

Basilevsky, A. T., Burba, G. A., Ivanov, M. A., Kryuchkov, V. P., Pronin, A. A., Bobina, V. P., Shashkina, V. P. & Head, J. W. 1997, Lunar Planet. Sci., 28, 75-76

Bindschadler, D. L., Shubert, G. & Kaula, W. M. 1992, J. Geophys. Res., 97, 13495-13532

Bullock, M. A. & Grinspoon, D. H. 1999, Icarus, submitted

Collins, G. C., Head, J. W., Basilevsky, A. T. & Ivanov, M. A. 1999, J. Geophys. Res., submitted

Ghent, R. R. & Hansen, V. 1999, Icarus 139, 116-136

Gilmore, M. S., Ivanov, M. A., Head, J. W. & Basilevsky, A. T. 1997, J. Geophys. Res., 102, 13,357-13,368

Gilmore, M. S., Collins, G. C., Ivanov, M. A., Marinangeli, L. & Head, J. W. 1998, J. Geophys. Res., 103, 16,813-16,840

Guest, J. E. & Stofan, E. R. 1999, Icarus, 139, 55-66

Hansen, V. L. & Willis, J. J. 1996, Icarus, 123, 296-312

Hansen, V. L. & Willis, J. J. 1998, Icarus, 132, 321-343

Hauck, S. A., Phillips, R. J. & Price, M. H. (1998) J. Geophys. Res., 103, 13635-13642

Head, J. W. & Basilevsky A. T. 1998, Geology, 26, 35-38

Herrick, R. R. & Sharpton, V. L. 1999, Icarus, submitted.

Ivanov, M. A. & Basilevsky, A. T. 1993 Geophys. Res. Lett., 20, 2579-2582

Ivanov, M. A. & Head, J. W. 1998, Lunar and Planetary Science, # 1261

McGill, G. E. 1993, Geophys. Res. Lett., 20, 2407-2410

McKinnon, W. B., Zahnle, K. J., Ivanov, B. A. & Melosh, H. J. 1997, in: Venus II, edited by S. W. Bougher, D. M. Hunten, and R. J. Phillips, 969-1014 (Univ. of Ariz. Press, Tuscon)

Namiki, N. & Solomon, S. C. 1994, Science, 265, 929-933

Parmentier, E. M. & Hess, P. C. 1992, Geophys. Res. Lett., 19, 2015-2018

Phillips, R. J. & Hansen, V. L. 1998, Science, 279, 1492-1497

Price, M. & Suppe, J. 1994, Nature, 372, 756-759

Schaber, G. G., Strom, R. G., Moore, H. J., Soderblom, L. A., Kirk, R. L., Chadwick, D. J., Dawson, D. D., Gaddis, L. R., Boyce, J. M. & Russell, J. 1992, J. Geophys. Res., 97, 13,257-13,302

Solomon, S. C., Bullock, M. A. & Grinspoon, D. H. 1998, Lunar Plan. Sci. Conf., 29, Abstract #1624 (CD-ROM)

Solomotov, V. S. & Moresi, L. -N. 1996, J. Geophys. Res., 101, 4737-4753

Turcotte, D. L. 1993, J. Geophys. Res., 98, 17061-17068

Turcotte, D. L., Morein, G., Roberts, D. & Malamud, B. D. 1999, Icarus, 139, 49-54

3. MARS ATMOSPHERE

(Contributed by Barney J. Conrath, Center for Radiophysics and Space Research, Cornell University, USA)

The Mars Global Surveyor (MGS) spacecraft placed in orbit about Mars 11 September 1997, and the Pathfinder lander, which arrived at Mars 4 July 1997, have obtained a large body of new information about the Martian atmosphere. Ongoing monitoring programs from ground-based observatories and the Hubble spacecraft also have continued to add to our understanding. Instrumentation carried on MGS has permitted characterization of the atmospheric thermal structure over essentially a complete Martian year, and has provided significant new data on condensation clouds and the behavior of atmospheric dust. During its descent to the surface of Mars, Pathfinder provided a detailed temperature profile. On the surface, its camera recorded data that will help to refine our understanding of the visible optical properties of the atmospheric dust. Earth-based observations of the latitude and local time behavior of the atmospheric column abundance of water vapor have continued, and the Hubble WFPC has been used to track the behavior of dust and condensation clouds. By far the most extensive new atmospheric data sets are those from MGS; consequently, this report will focus primarily on those results.

During its first two years of operation in orbit around Mars, the MGS Thermal Emission Spectrometer (TES) (Christensen et al. 1998) obtained almost 20 million thermal emission spectra. These have provided information on atmospheric thermal structure, dust, and water ice clouds. The seasonal evolution of the zonal mean meridional temperature structure from the surface to approximately 30 kilometers has been obtained, along with the associated thermal winds, for over one Martian year, providing strong observational constraints for the Mars General Circulation Models. Temperatures are generally found to depart significantly from radiative equilibrium, indicating strong modifications of the thermal structure by dynamical processes. Under solstice conditions, the temperatures at all levels are found to increase monotonically toward the summer pole with a strong polar front in the winter hemisphere associated with an intense circum-polar vortex. The solstice results show evidence for a strong cross-equatorial meridional (Hadley) circulation, much deeper and more extensive in latitude than that found in the terrestrial atmosphere. This

difference between planets is believed to be at least partly due to the lack of a large thermal reservoir (ocean) on Mars. Results from both equinox periods show some hemispheric asymmetry with stronger latitudinal gradients in the Northern Hemisphere in both cases, indicating zonal (eastward) winds almost twice as strong in the north as in the south.

The MGS TES instrument also provided maps of the 9-micrometer atmospheric dust optical depth. The occurrence of a strong regional dust storm in the Noachis Terra region during Southern Hemisphere spring seasonal conditions provided a unique opportunity to study the genesis, growth, and decay of such an event and to document its effects on the global thermal structure and dynamics. A gradual increase in atmospheric dust content was observed throughout the Southern Hemisphere, followed by a rapid increase localized in the Noachis region. Although heavy dust loading remained confined in the south, increased temperatures were observed aloft at high northern latitudes within approximately one day of the onset of the intense phase of the storm. This temperature increase is attributed to compressional warming in the descending branch of the cross-equatorial Hadley circulation, which rapidly intensified in response to atmospheric absorption of solar energy by dust in the Southern Hemisphere. These observations demonstrate the strong global thermal and dynamic response of the atmosphere to dust storm activity, even when the storm remains localized. In addition, numerous small dust storms were observed by both TES and the MGS imaging system (MOC), especially near the edge of the retreating south polar cap in southern summer (Malin et al. 1998). The Imager for Mars Pathfinder (IMP) solar images have been used to infer visible and near-IR dust optical depths of 0.4-0.5 during the late Northern Hemisphere summer while mean particle radii of 1.5-2.0 micrometers have been inferred from images of the Martian sky. These results are similar to those obtained with the Viking landers under similar conditions (Smith & Lemmon 1999).

While the TES measurements have provided very extensive spatial and temporal coverage of atmospheric temperatures with modest vertical resolution, radio occultation measurements from MGS have yielded complementary high vertical resolution temperature measurements over the same altitude range, but with limited spatial coverage. In addition, the occultation measurements yield pressure determinations, permitting direct estimates of gradient winds. Using this technique, a low altitude westerly jet with speeds in excess of 30 m/s was observed at low southerly latitudes near southern summer solstice. This jet is produced by the cross-equatorial Hadley circulation, and may contribute to the genesis of dust storms.

Accelerometer measurements from Mars Pathfinder, obtained as it descended through the atmosphere, provided detailed profiles of density, pressure and temperature from an altitude of 140 km down to about 9 km (Magalhaes et al. 1999). Wave activity is evident in the temperature profile at most levels similar to that observed in the Viking descent profiles.

During the aerobraking phase of the MGS mission, data from accelerometers carried on the spacecraft provided information on the behavior of atmospheric densities in the 110-150 km altitude region. This portion of the atmosphere was found to be unexpectedly variable on time scales of one day or less. Typical density variations of 70% were observed. Part of the variation appeared to be fixed in longitude and possibly correlated with the wavenumber 2 surface topography. With the onset of the Noachis Terra dust storm, the density at 130 km was observed to increase by a factor of approximately two in 2-3 days, and the density fluctuations increased in amplitude by about 200%. From these results, a new picture of the upper atmosphere has emerged in which the structure is dominated by large amplitude wave activity that is strongly coupled to the lower atmosphere.

TES measurements also provided new information on the atmospheric thermal tides. Diurnal and semi-diurnal modes have been observed, as well as non-migrating modes excited by interaction of the diurnal tide with large-scale topography. A diurnal mode with a phase reversal approximately two scale heights above the surface was observed for the first time at latitudes above 60 degrees south latitude. Such a mode is not predicted by classical tidal theory.

MGS has provided new observations of condensate clouds in the Martian atmosphere. The horizontal distribution of water ice clouds has been mapped in detail by MOC, and TES has provided thermal infrared optical depths of these clouds. With the onset of the Noachis dust storm, the ice clouds in the Southern Hemisphere vanished and reappeared with the storm decay. TES limb observations show stratified water ice clouds up to altitudes of 55 km. In the winter north polar region, a water ice haze is observed up to 40 km. Also in this region, the retrieved temperatures drop to the condensation point of carbon dioxide, and data from the laser altimeter experiment (MOLA) (Smith et al. 1998) suggest that CO_2 ice clouds are present.

This large body of new data has yet to be fully digested. The results, along with information to be obtained from additional spacecraft in the near future, should greatly enhance our understanding of the Martian atmosphere, especially its structure and dynamics, and the roles played by atmospheric dust and condensate clouds.

References

Christensen, P. R., Anderson, D. L., Chase, S. C., Clancy, R. T., Clark, R. N. , Conrath, B. J., Kieffer, H. H., Kuzmin, R. O., Malin, M. C., Pearl, J. C., Roush, T. L., & Smith, M. D. 1998, Science, 279, 1692-1698

Magalhaes, J. A., Schofield, J. T., & Seiff, A. 1999, J. Geophys. Res., 104, 8943-8955

Malin, M. C., Carr, M. H., Danielson, G. E., Davies, M. E., Hartmann, W. K., Ingersoll, A. P., James, P. B., Masursky, H., McEwen, A. S., Soderblom, L. A., Thomas, P., Veverka, J., Caplinger, M. A., Ravine, M. A., Soulanille, T. A., & Warren, J. L. 1998, Science, 279, 1681-1685

Smith, D. E., Zuber, M. T., Frey, H. V., Garvin, J. B., Head, J.W., Muhleman, D. O., Pettengill, G. H., Phillips, R. J., Solomon, S. C., Zwally, H. J., Banerdt, W. B., & Duxbury, T. C. 1998, Science, 279, 1686-1692

Smith, P. H., & Lemmon, M. 1999, J. Geophys. Res., 104, 8975-8985

4. GEOCHEMISTRY OF MARS

(Contributed by Heinrich Wänke, Max-Planck-Institut für Chemie, Mainz, Germany)

The Pathfinder mission yielded the first in situ analysis of the chemical composition of Martian rocks with the APX-spectrometer on the rover Sojourner. The data (Rieder et al. 1997) indicated that the soil on Mars might be chemically homogeneous on a global scale as the Pathfinder soil is chemically almost identical to that at Viking 1 and 2 sites. The rocks embedded in the soil at the Pathfinder site turn out to be rather similar to each other but very different compared to the soil. In contrast to the mafic character of the Martian soil and the Martian meteorites, the Pathfinder rocks are felsic rocks, rich in SiO_2 and K and low in Mg. Hence, the consensus generally reached after the Viking soil analyses of a rather primitive and mafic composition of the Martian surface has to be put into new perspective.

The Pathfinder data yield about 1 % K_2O for the rocks and 0.6 % for the soil samples. The determinations of the XRF-spectrometers on board of Viking 1 and 2 gave only upper limits of 0.15 % K_2O (Clark et al. 1982). There is no apparent explanation for this difference. Data on Mn and Cr proved that the Pathfinder rocks exhibit the same elemental characteristics as known from the study of Martian meteorites. For carbon only an upper limit of 0.8 wt.% was found for the soil.

The five rocks analyzed at the Pathfinder site (Barnacle Bill, Yogi, Wedge, Shark, and Half Dome) show sulfur concentrations between 0.3 and 1.6 %. This reflects the fact that all these rocks are partly covered by soil. Good linear regressions of the concentrations of each element versus sulfur were found and the composition of a "sulfur-free rock" calculated: Na_2O = 2.6 %, MgO = 1.8 %, Al_2O_3 = 10.6 %, SiO_2 = 62 %, Cl = 0.26 %, K_2O = 1.1 %, CaO = 7.3 %, TiO_2 = 0.6 %, Cr_2O_3 = 0.06 %, FeO = 13.2 % (all in weight %).

Both sulfur and chlorine dominate in the soil. But it became evident that even rocks with no adhering soil (sulfur-free rock) show enhanced chlorine concentrations of about 0.25 %. Such high values are outside the range observed in the terrestrial igneous rocks. It may be that the chlorine sits in veins due to infiltration of water from the early northern ocean. Pathfinder rocks compositionally match terrestrial andesites, this seems now even to be true for chlorine. On Earth chlorine in andesites (up to 0.15 %) is directly related to the involvement of seawater in their genesis. Is there an analogous mechanism indicated for the SiO_2 rich Martian rocks? (Wänke et al. 1999).

With the assumption that the soil data reflect the mean composition of the Martian surface, a mixing diagram with the mean composition of Pathfinder rocks as felsic end-members and the mean composition of all Martian meteorites as mafic end-member was derived (Wänke et al. 1999). Surprisingly good fits of the mixing lines were found for all elements. The mixing diagram indicates that the felsic component and the mafic component contribute about equally to the Martian soil. This might also reflect the abundance ratio of the two major provinces on the Martian surface. The southern highlands could be the home of the felsic, highly fractionated component while the mafic, more primitive component, is probably derived from the younger volcanic provinces like the Tharsis region.

The compositional difference of soil and rocks at the Pathfinder landing site is so large that it is clear that the soil cannot be made just by diminution of the rocks which are embedded in the soil. This even holds if one takes weathering and interaction with volcanic gases into account which are the source of sulfur and chlorine in the soil. Addition of an additional rock component rich in magnesium but lower in silicon and potassium is an unavoidable necessity. The Martian meteorites being highly variable in composition but generally mafic to even ultramafic might well represent such material. The compositional range of the Martian meteorites together with the composition of the Pathfinder rocks reflect the wide compositional variance of the Martian surface rocks (Fig. 1).

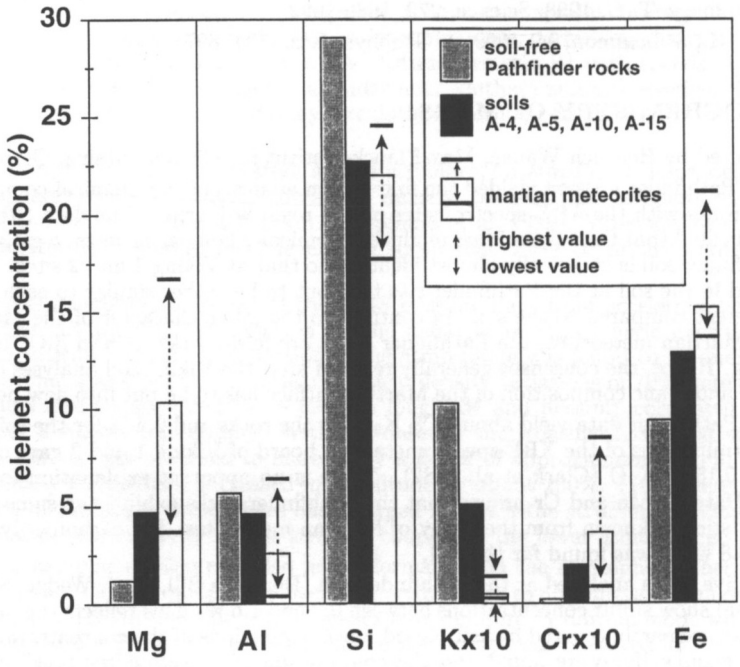

Figure 1 : Comparison between soil-free rock, soils and Martian meteorites

https://doi.org/10.1017/S0251107X00002662 Published online by Cambridge University Press

References

Clark, B. C., Baird, A. K., Weldon, R. J., Tsusaki, D. M., Schnabel, L., & Candelaria, M. P. 1982, J.Geophys. Res., 87, 10059-10067

Rieder, R., Economou, T., Wänke, H., Turkevich, A., Crisp, J., Brückner, J., Dreibus, G. & McSween Jr., H.Y. 1997, Science, 278, 1771-1774

Wänke H., Brückner, J., Dreibus, G., Lugmair, G.W., Rieder, R., & Economou, T. 1999, in : 5th International Conference on Mars, Abstract no. 6046 (Houston: Lunar & Planet. Inst.), (CD-ROM) LPI Contrib. 972

5. THE MOON

(Contributed by Carle M. Pieters, Department of Geological Sciences, Brown University, USA)

The last several years have been extremely exciting for studies concerning the Moon and its evolution. Two small missions, Clementine and Lunar Prospector, ended the decades-long drought of new data for the Moon. Clementine, which flew in 1994, was sponsored by the Ballistic Missile Defense Organization while NASA participated by providing Deep Space Network support. NASA and CNES also provided an international science team to enhance the return of scientific data. NASA subsequently supported data processing and production of useful Clementine data products. Lunar Prospector flew in 1998-1999 and was supported entirely by NASA as a Discovery Mission. Although the instruments aboard these orbital spacecraft were not the advanced sensors the science community has long awaited, they were quite capable and enormously productive. Data products from both missions continue to be processed; initial data are publicly available and can be found at:

http://www-pdsimage.jpl.nasa.gov/PDS/public/Atlas/Atlas.html

http://pds-geophys.wustl.edu/pds/clementine/

http://wundow.wustl.edu/lunarp/

Much of the new data (Nozette et al. 1994; Binder 1998) are global in nature and provide a perspective that allows several fundamental geophysical and compositional properties to be analyzed for the planetary body as a whole. The new global data include: 1) topography (e.g., Zuber et al. 1994), 2) extended visible multispectral imagery (e.g., McEwen & Robinson 1997), 3) gamma-ray spectroscopy (Lawrence et al. 1998; 1999), and 4) neutron spectroscopy (Feldman et al. 1998a,b). Although the spatial resolution of different data sets range from 150 m to 150 km, their near-global coverage allows different properties to be linked and intercompared. Some of the more useful global data products that have been derived from these measurements include estimates of crustal thickness and maps of radiogenic elements, iron, and hydrogen abundances.

The pulse of new data immediately highlighted our ignorance of several fundamental issues about the Moon and continues to spark renewed interest in processes of the early solar system for which the Moon is well positioned to illuminate. Although numerous focused studies have enriched the research literature as a result, highlighted here are some of the broad results that can be considered recent scientific breakthroughs.

5.1. Water Ice (H) at the Poles

It is well known that the Moon is very dry and devoid of volatiles. Nevertheless, the Moon has experienced the same flux of cometary impacts as the Earth. It has long been hypothesized that some of the water molecules released in the process could eventually enter permanently shadowed areas in some craters near the lunar poles and would not be able to escape. Transient lunar water produced during soil formation by the reduction of lunar soil components with solar wind hydrogen could similarly migrate and be trapped at the poles. The Clementine radar experiment (Nozette et al. 1996) suggested the existence of

water ice at the lunar south pole. The Lunar Prospector neutron spectrometer experiment provided concrete evidence for the existence of abundant H at the poles, with the preferred interpretation that substantial deposits of water ice exist in the permanently shadowed areas of both poles (Feldman et al. 1998a, b).

5.2. South Pole-Aitken Basin Compositional Anomaly

When Galileo flew by the Earth/Moon system on its way to Jupiter it obtained the first photometric quality multispectral images of part of the lunar farside. The lighting conditions allowed both albedo and extended visible color to be radiometrically measured for half of the farside. The results were astounding. The existence of an enormous basin centered on the farside extending from the equator (near the crater Aitken) to the south pole was confirmed. The possible presence of this giant lunar basin, called South Pole-Aitken Basin [SPA] for lack of a better name, was suggested in early lunar exploration, but it remained unconfirmed and is rarely found on lunar maps. Although there are only a few small mare ponds present, the central portion of the SPA basin was seen to have a low albedo and a mafic (iron-rich) signature (Belton et al. 1992). Clementine topography later showed the 2500 km diameter SPA to contain some of the deepest regions on the Moon, whereas areas to the north of the basin exhibited some of the highest elevations (a 16 km difference), making SPA perhaps the largest basin in the solar system (Zuber et al. 1994; Spudis et al. 1994). Recent analysis of compositional data from Clementine and Lunar Prospector clearly indicates SPA represents an enormous unsampled iron-rich anomaly. Although the size of the basin suggests significant amounts of mantle should be exposed by the basin-forming event early in lunar evolution, the limited compositional information that can be derived from existing data have not conclusively resolved the proportions of lower crust and/or mantle currently exposed (Pieters et al. 1997; Lucey et al. 1998).

5.3. Magma Ocean and Distribution of Anorthosite

The magma ocean hypothesis for formation of the primitive anorthositic lunar crust and mafic mantle has generally stood the test of time. The relatively simple mineralogy of the Moon allows plagioclase anorthosite to be readily detected with Clementine multispectral data by the absence of iron-bearing species. The new Clementine analyses have strengthened the magma ocean hypothesis with a global perspective but have also raised new questions in understanding the details of global crustal evolution. Both compositional estimates of surface soils (Lucey et al. 1995) as well as mineralogical analyses of crustal stratigraphy (Tompkins & Pieters, 1999) document the preponderance and distribution of anorthosite across the lunar highlands as well as the presence of diverse relationships between anorthosite and more mafic-bearing species of the lunar crust.

5.4. Imbrium Hot Spot

Materials enriched in "KREEP" (potassium, rare earth elements, and phosphorous) have been studied in the lunar samples and are believed to represent some of the last material to crystallize during formation of the crust and mantle. The presence of radiogenic elements is a good marker for KREEP and the Lunar Prospector gamma-ray spectrometer data provide the first global assessment of where this key crustal component is located on the surface of the Moon. Much to everyone's surprise, the abundance of radiogenic materials appears to be associated almost exclusively with the Imbrium basin and its deposits (Lawrence et al. 1998; 1999). This apparently lopsided distribution of KREEP remains unexplained, but clearly must have occurred early in lunar crustal evolution.

5.5. Advanced Laboratory Technology

In parallel with renewed exploration of the Moon using small spacecraft, the technology available in earth-based laboratories has expanded dramatically in the last decade and

several micro-analytical techniques are being used to probe deeper into extracting new information from the valuable collection of curated lunar samples. One example of an area of particular broad and insightful research that has made recent progress is studies of space weathering processes and effects (formation and distribution of nano-phase iron, elemental fractionation by sputtering and vapor deposition, mineral fractionation by physical processes, etc.). Until additional samples are returned from other planetary bodies, lunar samples are our only resource to understand small-scale processes that occur on airless bodies.

References

Belton, M. J. S. et al. 1992, Science, 255, 570-576

Binder, A. B. 1998, Science, 281, 1475-1476

Feldman, W. C., Barraclough, B. L., Maurice, S., Elphic, R. C., Lawrence, D. J., Thomsen, D., & Binder, A. B. 1998a, Science, 281, 1489-1493

Feldman, W. C., Maurice, S., Binder, A. B., Barraclough, B. L., Elphic, R. C., & Lawrence, D. J. 1998b, Science, 281, 1496-1500

Lawrence, D. J, Feldman, W. C., Barraclough, B. L., Binder, A. B., Elphic, S. Maurice, R. C., & Thomsen, D. R. 1998, Science, 281, 1484-1489

Lawrence, D. J., Feldman, W. C., Barraclough, B. L., Binder, A. B., Elphic, R. C., Maurice, S., Miller, M. C., & Prettyman, T. G. 1999, Geophys. Res. Let., in press

Lucey P. G., Taylor, G. J., Hawke, B. R., & Spudis, P. D. 1998, J. Geophys Res., 103, 3701-3708

Lucey P. G., Taylor, G. J., & Malaret, E. 1995, Science, 268, 1150-1153

McEwen, A. S., & Robinson, M. S. 1997, Advances in Space Research, Vol 19, No. 10, 1523-1533

Nozette, S. et al. 1994, Science, 266, 1835-1839

Nozette S., Lichtenberg, C. L., Spudis, P., Bonner, R., Ort, W., Malaret, E., Robinson, M., & Shoemaker, E. 1996, Science, 274, 1495-1498

Pieters, C. M., Tompkins, S., Head, J. W., & Hess, P. C. 1997, Geophys. Res. Lett., 24, 1903-1906

Spudis P. D., Reisse, R. A., & Gillis, J. J. 1994, Science, 266, 1848-1851

Tompkins, S., & Pieters, C. M. 1999, Meteoritics & Planetary Science, 34, 25-41

Zuber, M. T., Smith, D. E., Lemoine, F., & Neumann, G. A. 1994, Science, 266, 1839-1843

6. PLANETARY ATMOSPHERES: NEW RESULTS FROM ISO

(Contributed by Thérèse Encrenaz, Observatoire de Paris, Meudon, France)

The Infrared Space Observatory (ISO) has significantly contributed to our knowledge of planetary atmospheres over the period 1996-1999. ISO, operated by the European Space Agency, was launched on November 17, 1995 and observed astronomical sources from Earth orbit until April 8, 1998. ISO consisted of a 60-cm helium cooled telescope (Kessler et al. 1996), equipped with 4 focal plane instruments: a camera (CAM, 2.5-17 μm; Césarsky et al. 1996), a photometer (PHT, 2-200 μm; Lemke et al. 1996) and 2 spectrometers, SWS (de Graauw et al. 1996) and LWS (Griffin et al. 1996) covering the range 2.3-200 μm with a spectral resolving power ranging from 200 (LWS grating mode) to 30000 (SWS Fabry-Perot mode).

The solar-system program of ISO included observations of Mars, the giant planets, satellites, asteroids, comets and the zodiacal light. The SWS instrument was especially successful for the study of planetary atmospheres, both in its grating mode (R=1500-2000) and its Fabry-Perot mode. Major results include (1) a new determination of the deuterium abundance in the giant planets; (2) the unexpected discovery of an external oxygen source

in the stratospheres of the giant planets; (3) the detection of several new hydrocarbons in these stratospheres; (4) the detection of H_2O in the deep troposphere of Saturn; (5) the study of the thermal structure of the giant planets, the vertical distributions of their gaseous constituents, and their cloud composition.

6.1. D/H in the giant planets

The detection of infrared rotational lines of HD allowed for the first time a simultaneous determination of D/H in the four giant planets (Encrenaz et al. 1996; Griffin et al. 1996; Lellouch, 1999; Feuchtgruber et al. 1999a). The D/H value was found to increase with heliocentric distance from 1.8 10^{-5} (+1.1,-0.5) in the case of Jupiter to 6.5 (+2.5,-1.5) 10^{-5} in the case of Neptune. In addition, the D/H value in Jupiter was found to be fully consistent with the jovian value derived from Galileo, and in very good agreement with the protosolar value of D/H. These results confirm that Jupiter seems to be indeed representative of the primordial solar nebula; they also support the nucleation model which predicts a deuterium enrichment in the icy giants Uranus and Neptune, due to the larger mass fraction of their initial icy cores.

6.2. The external oxygen source

A major result from ISO was the unexpected detection of water vapor in the high stratospheres of the four giant planets (Feuchtgruber et al. 1997, 1999b), through the identification of several rotational transitions. In addition, carbon dioxide was also detected in Jupiter, Saturn and Neptune. Because of the low temperature of the tropopause, H_2O (as well as CO_2 in the case of Uranus and Neptune) cannot be transported from the interior and has to be of external origin. The origin of this external oxygen source could be either an interplanetary micrometeoritic flux or a local source coming from the rings and/or the icy satellites.

6.3. Detection of new hydrocarbons

Methane photolysis is known to be very active in the giant planets. Among the hydrocarbons whose presence is expected from photochemical models, ethane C_2H_6 and acetylene C_2H_2 were known to be present in the stratospheres of all four planets, with the exception of C_2H_6 on Uranus. ISO observations have added several new detections to the hydrocarbon list. C_3H_4 (methylacetylene), C_4H_2 (diacetylene), C_6H_6 (benzene) and the CH_3 methyl radical were all detected in Saturn (de Graauw et al. 1997; Bézard et al. 1998, 1999a); CH_3 and C_2H_4 (ethylene) were detected in Neptune (Bézard et al. 1999b; Schulz et al. 1999). All these results provide new constraints on photochemical models and lead to a better understanding of the complex photochemistry of the giant planets.

6.4. Detection of tropospheric water in Saturn

As in the case of Jupiter, the infrared spectrum of Saturn exhibits a window, around 5 microns, where the flux comes from deep atmospheric levels, thus allowing the deep troposphere to be probed, down to a pressure level of a few bars, in specific cloud-free regions ("hot spots"). Phosphine PH_3 and deuterated methane CH_3D were known to be the most important absorbers, while weaker signatures were identified as due to carbon monoxide CO, germane C_2H_4 and arsine AsH_3. The ISO spectrum of Saturn has shown for the first time the signature of H_2O (de Graauw et al. 1997), which had been previously detected in Jupiter only. An interesting result is that water is strongly undersaturated, which is also what is observed in the case of Jupiter. This might imply some similarities between the circulation mechanisms of both planets, although significant differences appear between the hot spots distributions of both planets.

6.5. Atmospheric structure

In the case of Jupiter and Saturn, the thermal profiles of the giant planets have been retrieved from the use of the infrared bands of CH_4, whose mixing ratio is constant with height (de Graauw et al. 1997). In addition, fluorescence emission of methane has been detected on both planets in the near-infrared range, leading to a determination of their eddy diffusion coefficient (Drossart et al. 1999). In the case of Uranus, this parameter was retrieved from a study of an infrared C_2H_2 band (Encrenaz et al. 1998). Finally, in the case of Jupiter, information was obtained on the vertical distribution of ammonia and on the $^{14}N/^{15}N$ ratio (Fouchet et al. 1999), as well as the nature of the NH_3 ice cloud (Brooke et al. 1998).

References

Bézard, B., Feuchtgruber, H., Moses, J.L., & Encrenaz, Th. 1998, A&A334, L41-L44.

Bézard, B., Romani, P.N., & Encrenaz, Th. 1999a, ApJ, 515, 868-872.

Bézard, B., Feuchtgruber, H., & Encrenaz, Th. 1999b, ESA SP-427, 153-156.

Brooke, T.Y., Knacke, R.F., Encrenaz, Th., Drossart, P., Crisp, D., & Feuchtgruber, H. 1998, Icarus, 136, 1-13.

Césarsky, C. et al. 1996, A&A, 315, L32-L37.

Drossart, P., Fouchet, Th., Crovisier, J., Lellouch, E., Encrenaz, Th., Feuchtgruber, H., & Champion, J.P. 1999, ESA SP-427, 169-172

Encrenaz, Th. et al. 1996, A&A, 315, L397-L400

Encrenaz, Th. et al. 1998, A&A, 333, L43-L46

Feuchtgruber, H., Lellouch, E., de Graauw, Th., Bézard, B., Encrenaz, Th., & Griffin, M. 1997, Nature, 389, 159-162

Feuchtgruber, H. et al. 1999a, ESA SP-427, 133-136

Feuchtgruber, H., Lellouch, E., Bézard, B., Encrenaz, Th., de Graauw, Th., & Davis, G. R. 1999b, A&A, 341, L17-L21

Fouchet, Th., Lellouch, E., Bézard, B., Encrenaz, Th., Drossart, P., Feuchtgruber, H., & de Graauw, Th. 1999b, Submitted to Icarus

de Graauw, Th. et al. 1996, A&A, 315, L49-L54

de Graauw, Th. et al. 1997, A&A, 321, L13-L16

Griffin, M. J. et al. 1996, A&A, 315, L389-L392

Kessler, M. F. et al. 1996, A&A, 315, L27-L31

Lellouch, E. 1999, ESA SP-427, 125-132

Lemke, D. et al. 1996, A&A, 315, L64-L70

Schulz, B., Encrenaz, Th., Bézard, B., Romani, P., Lellouch, E., & Atreya, S. K. 1999, A&A, in press

7. GALILEO PROBE: LATEST RESULTS

(Contributed by Sushil K. Atreya, University of Michigan, and Richard E. Young, NASA Ames Research Center, USA)

Nearly six years after its launch, the Galileo spacecraft released Galileo Probe toward Jupiter on July 13, 1995. Five months later, on December 7, 1995, Galileo Probe became the first probe ever to enter into a giant planet. It entered the atmosphere of Jupiter at a planetocentric latitude of 6.53°N and a System III longitude of 0.94°W (Young 1998). On the same day, after the Probe entry, Galileo Orbiter, the second part of the spacecraft, was placed into its initial orbit around Jupiter. For 58 minutes, the Probe transmitted data from its various instruments to the Orbiter for relay to the earth. Measurements were carried out from an altitude of 1000 km above 1-bar to a depth of 132 km where a pressure

of 22 bars was reached, thus surpassing the expectations of a 40-minute/10-bar nominal mission. The Galileo Orbiter mission continues to this day.

The Probe made the first in situ measurements of the chemical composition, cloud structure, net radiative flux, winds, temperature, pressure, turbulence, and lightning in the atmosphere of Jupiter. In addition, the probe-orbiter radio signal was studied to infer atmospheric properties. The Probe Neutral Mass Spectrometer (GPMS) made the first direct and in situ measurement of HD in Jupiter's atmosphere, thereby determining the hydrogen isotopic ratio on Jupiter. A value of $D/H=2.6x10^{-5}$ was measured (Mahaffy et al. 1998a). This measurement is significant since it represents the protosolar D/H, as the sun's deuterium has long since been converted to helium through thermonuclear processes. The Helium Abundance Detector and the GPMS both made an accurate measurement of $He/H_2=0.157$, which is 0.81 x solar (von Zahn et al. 1998; Niemann et al. 1998). The atmospheric depletion of helium is attributed to the loss of this species by condensation in Jupiter's interior. All other noble gases were also measured for the first time in Jupiter's atmosphere. The GPMS determined a neon elemental ratio of 0.1 x solar (Niemann et al. 1998). The depletion of neon is most likely the result of differentiation of this gas into helium droplets which carry neon with them as they precipitate to the core of Jupiter (Roulston & Stevenson 1995). The elemental ratios of argon, xenon and krypton are found to be between a factor of 2-3 greater than their solar values (Mahaffy et al. 1998b).

Sulfur was detected for the first time in the unperturbed Jovian atmosphere. The GPMS measured $H_2S/H_2=2.5$ x solar at a depth of 15 bars where it leveled off (Niemann et al. 1998). However, in the upper parts of the atmosphere, this species was highly depleted and subsaturated, but its mixing ratio gradually built up with depth. A similar behavior was seen in ammonia. The Net Flux Radiometer (NFR) on the Probe (Sromovsky et al. 1998) and the Orbiter Near Infrared Mapping Spectrometer (NIMS, Irwin et al. 1998) both derived greatly depleted amounts of ammonia in the upper parts of the atmosphere. Deeper in the atmosphere, the NFR data are consistent with an ammonia mixing ratio of 1-2 x solar between 3-6 bars. The attenuation of the 21.6 cm radio transmission from the probe to the orbiter was analyzed to yield an ammonia mixing ratio with depth (Folkner et al. 1998). A steady value of 3.6 x solar was reached at the 8-bar level. Although the behavior of water vapor was similar to that of H_2S and NH_3 - depleted above and increasing with depth - its mixing ratio even at the deepest level probed (21 bars) was subsolar and perhaps still increasing (Niemann et al. 1998). The NIMS data are also consistent with highly subsaturated water down to the level of the validity of their data (approximately 8 bars, Roos-Serote et al. 1998).

Contrary to expectations, only very thin wispy clouds were detected in the Galileo Probe entry region. The Nephelometer detected a tenuous cloud at 1.3 bar, an equally tenuous one at 0.5 bar (also seen by NFR), perhaps a very thin condensate layer at 1.6 bar, and some particles down to 4 bars (Ragent et al. 1998). The cloud layers at 0.5 bar, 1.3 bar and 1.6 bar are consistent with the clouds of NH_3-ice, NH_4SH-ice and H_2O-ice, respectively, considering the abovementioned depleted abundances of these condensibles in the Probe entry site (Atreya et al. 1999). The extreme dryness of the Probe region has been variously attributed to the nature of this region. The Probe descended into a 5-micron hotspot, a region of downwelling (Orton et al. 1998). Local meteorology, in the form of downdrafts, has been invoked by several groups (Atreya et al. 1997; Owen et al. 1997; Showman & Ingersoll 1998; Baker & Schubert 1998) to explain the depletion of and gradient in the mixing ratios of the condensible volatiles in the Probe region. Although appealing, the models require considerable work before they could satisfactorily explain the observed behavior.

The supersolar values of C, S, N, and the heavy noble gases measured by the Probe provide unprecedented constraints to the models of the formation of Jupiter and the evolution of its atmosphere. It is inevitable that the conventional icy planetesimal model will have to be refined as a result (Atreya et al. 1999).

The probe Atmospheric Structure Instrument (ASI) determined the thermal structure of the upper atmosphere from accelerometer readings during the high speed probe entry portion of the mission, from about 1000 km altitude (measured from the 1 bar pressure surface) to approximately 21 km altitude (corresponding to about 0.4 bars), at which point the descent portion of the probe mission began and T, p were measured directly. The probe transmitted data to an altitude of -132 km corresponding to a pressure of 22 bars (Seiff et al. 1998). The upper atmosphere ASI results showed the existence of large vertical temperature gradients, reaching a maximum slightly over 5 K/km at about 425 km altitude, but with the vertical gradients becoming small at higher altitudes. Temperature was determined to be 900 $\pm$ 40 K at 800 km, with the uncertainty rapidly decreasing with decreasing altitude. Superposed on the mean temperature profile are temperature oscillations reaching several tens of degrees K, indicative of the existence of atmospheric waves, probably gravity waves. In the deeper atmosphere below the 0.4 bar pressure level, temperature as a function of pressure was measured to be very close to that predicted by a dry adiabat.

Doppler tracking of the probe, both from the Galileo orbiter (Atkinson et al. 1998) and from the ground using the VLA (Folkner et al. 1997), established for the first time that, at least at the probe entry site, the zonal (east-west) winds previously inferred from cloud tracking extend into the deep atmosphere, at least as deep as the approximately 22 bars reached by the probe (Atkinson et al. 1998). There is substantial vertical variation in the winds between the start of probe descent measurements at 0.4 bars to about 4 bars. The winds near 0.4 bars are subject to significant error because of orbiter-probe geometry, and derived values range from 70 to 120 ms^{-1}. At pressures near and above 4 bars, the winds as determined by probe tracking from the orbiter level off to a more or less constant speed of about 170 ms^{-1} (Atkinson et al. 1998). The VLA measurements (Folkner et al. 1997), which extend to pressures just above 4 bars, reach somewhat higher wind speeds, about 200 ms^{-1}. Analysis of accelerometer data from the ASI has yielded wind profiles that are basically consistent, to within the ranges given above, with the Doppler tracking (Seiff et al. 1997).

The fact that the winds extend well below both the region of clouds and the depth to which solar energy penetrates to any significant degree (cf Sromovsky et al. 1998) probably implies that Jupiter's internal heat flux provides the basic energy source for the winds.

The Galileo probe was equipped to search for lightning events. The probe had two kinds of lightning detection sensors: optical sensors located 180° from each other about the spin axis of the probe, and a radio frequency antenna. Optical events were recorded during probe descent, but are not attributed to lightning (Lanzerotti et al. 1996; Rinnert et al. 1998). Radio frequency (RF) wave forms indicated that the probe descended through a region devoid of lightning within at least 104 km from the probe entry site, the most probable distance being about 1.5 x 10^4 km (Rinnert & Lanzerotti 1998). In other words, the nearest lightning was probably about 12° away on a surface with radius of 1 jovian radius. The source spectrum of RF signals was dominated by low frequencies, in contrast to terrestrial lightning source spectra which are wideband and relatively flat. The spectral shape of the RF waveforms could not be attributed to frequency dependent absorption of RF signals (Rinnert & Lanzerotti 1998). Thus, if the RF source is lightning, the lightning pulses must be relatively long, the order of a few hundred seconds. The average dissipated energy is 10^{12} J, about 1000 times larger than on Earth (Rinnert et al. 1998; Rinnert & Lanzerotti 1998). Attributing the RF signals to lightning, the detected rate of occurrence is about 0.07 km^{-2} yr^{-1}, about 0.01 times the average terrestrial rate.

References

Atkinson, D. H., Pollack, J. B., & Seiff, A. 1998, J. Geophys. Res., 103, 22857-22889

Atreya, S. K., Wong, M. H., Owen, T. C., Niemann, H. B., & Mahaffy, P. R. 1997, in Three Galileos: The Man, The Spacecraft, The Telescope, eds. C. Barbieri et al. (The Netherlands: Kluwer Academic Publishers, Dordrecht) 249-260

Atreya, S. K., Wong, M. H., Owen, T. C., Niemann, H. B., Mahaffy, P. R, de Pater, I., Drossart P., & Encrenaz, Th. 1999, Planet. Space Sci., in press

Baker, R. D., & Schubert, G. 1998, Icarus, 136, 340-343

Folkner, W. M., Preston, R. A., Border, J. S., Navarro, J., Wilson, W. E., & Oestreich, M. 1997, Science, 275, 644-646

Folkner, W. M., Woo, R., & Nandi, S. 1998, J. Geophys. Res., 103, 22847-22856

Irwin, P. G. J. et al. 1998, J. Geophys. Res., 103, 23001-23022

Lanzerotti, L. J., Rinnert, K., Dehmel, G., Gliem, F. O., Krider, E. P., Uman, M. A., & Bach, J. 1996, Science, 272, 858-860

Mahaffy, P. R., Donahue, T. M., Atreya, S. K., Owen, T. C., & Niemann, H. B. 1998a, Space Science Rev., 84, 251-263

Mahaffy, P. R., Niemann, H. B., Alpert, A., Atreya, S. K., Donahue, T. M., & Owen, T. C. 1998b, Bull. Am. Astron. Soc., 30, 1066, Presented at the 30th DPS/AAS meeting, Madison, WI, October

Niemann, H. B., Atreya, S. K., Carignan, G. R., Donahue, T. M., Haberman, J. A., Harpold, D. N., Hartle, R. E., Hunten, D. M., Kasprzak, W. T., Mahaffy, P. R., Owen, T. C., & Way, S. H. 1998, J. Geophys. Res., 103, 22831-22846

Orton, G. S., Fisher, B. M., Baines, K. H., Stewart, A. T., Friedson, A. J., Ortiz, J. L., Marinova, M., Ressler, M., Dayal, A., Hoffmann, W., Hora, J., Hinkley, S., Krishnan, V., Masanovic, M., Tesic, J., Tziolas, A., & Parija, K.C. 1998, J. Geophys. Res., 103, 22791-22814

Owen, T. C., Atreya, S. K., Mahaffy, P., Niemann, H. B., & Wong, M. H. 1997, in Three Galileos: The Man, The Spacecraft, The Telescope, eds. C.Barbieri et al. (The Netherlands: Kluwer Academic Publishers, Dordrecht) 289-297

Ragent, B., Rages, K. A., Knight, T. C. D., Arvin, P., & Orton, G. S. 1998, J. Geophys. Res., 103, 22891-22909

Rinnert, K., Lanzerotti, L. J., Uman, M. A., Dehmel, G., Gliem, F. O., Krider, E. P., & Bach, J. 1998, J. Geophys. Res., 103, 22979-22992

Rinnert, K., & Lanzerotti, L. J. 1998, J. Geophys. Res., 103, 22993-22999

Roos-Serote, M., Drossart, P., Encrenaz, Th., Lellouch, E., Carlson, R., Baines, K., Kamp, L., Orton, G., Muhlman, R., Calcutt, S., Irwin, P., Taylor, F., & Weir, A. 1998, J. Geophys. Res., 103, 23023-23042

Roulston, M. S., & Stevenson, D. J. 1995, (abstract) EOS 76, F343

Seiff, A., Schubert, G., Knight, T. C. D., Blanchard, R. C., Kirk, D. B., Atkinson, D., Mihalov, J., & Young, R. E. 1997, Nature, 388, 650-652

Seiff, A., Kirk, D. B., Knight, T. C. D., Young, R. E., Mihalov, J. D., Young, L. A., Milos, F. S., Schubert, G., Blanchard, R. C., & Atkinson, D. 1998, J. Geophys. Res., 103, 22857-22889

Showman, A. P., & Ingersoll, A. P. 1998, Icarus, 132, 205-220

Sromovsky, L. A., Collard, A. D., Fry, P. M., Orton, G. S., Lemmon, M. T., Tomasko, M. G., & Freedman, R. S. 1998, J. Geophys. Res., 103, 22929-22977

von Zahn, U., Hunten, D. M., & Lehmacher, G. 1998, J. Geophys. Res., 103, 22815-22829

Young, R. E. 1998, J. Geophys. Res., 103, 22775-22790

8. PLANETARY RINGS

(Contributed by Joseph A. Burns, Cornell University, Ithaca, USA)

Significant progress toward understanding planetary rings has been accomplished during the last three years. Galileo observations of Jupiter's rings have led to a new model for that ring's operation; measurements of crossings of Jupiter's and Saturn's ring plane by ground-based telescopes and the Hubble Space Telescope have provided new insights about ring structure. Theorists, motivated in part to interpret these results but also to prepare for spacecraft visits to ring systems, have also been busy during the triennium.

Galileo, returning the first spacecraft measurements (imaging, infrared and dust instruments) of a ring system in a decade, has corroborated many of Voyager's findings but has also found new things. Jupiter's main ring, which is perfectly circumscribed by the orbit of the small moon Adrastea, has a brightness decrease of 10-20% surrounding Metis's orbit, about two-thirds of the way out in the ring; brightness variations of +/- 10% are visible in the central main ring. Detected for the first time in back-scattered light (de Pater et al. 1999), the halo starts near an electromagnetic resonance and contains smaller particles than the main ring. Galileo images (Ockert-Bell et al. 1999) reveal that Jupiter's gossamer ring – previously seen only in its Voyager discovery image – is in fact two faint rings that are apparently bounded by the orbits of a pair of small ring-moons, Amalthea and Thebe. Very faint material continues past Thebe's orbit at 222,000 km, blending into the background at ~250,000 km. When viewed nearly edge-on, the gossamer rings have a rectangular end-shape with enhanced intensities along the top and bottom edges. The gossamer rings have thicknesses that are comparable to the maximum elevations of their bounding satellites off Jupiter's equatorial plane. Burns et al. (1999) argue that the unique morphology of the gossamer rings can be generated if the ring particles are collisional ejecta evolving radially inward (apparently due to Poynting-Robertson drag) from the source satellites; Jupiter's main ring may also be produced similarly by debris lost from the ring-moons Adrastea and Metis.

Impacts account for other ring phenomena. Galileo's dust detector (Grun et al. 1998) has identified ejecta coming off the Galilean satellites and has demonstrated that the motion of Jovian circumplanetary dust carries a strong signature of periodic electromagnetic forces from Jupiter's spin and Io's orbit. Voyager images show that sections of Saturn's F ring brighten abruptly, likely due to debris thrown off during impacts of cm-sized meteoroids. Cuzzi and Estrada (1998) claim that color variations that were earlier carefully measured across Saturn's rings result from the contamination of the ring by dark impactors.

Modelling studies have characterized "ring" environments that will soon be visited by spacecraft. Nozomi, the Japanese mission now heading to Mars has engendered many studies of a ring not yet seen, the debris tori from Phobos and Deimos (e.g., Krivov & Hamilton 1997). Observations during ring-plane crossings of Saturn's faint E and G rings, as well as reinterpretations of Voyager imaging and plasma data, have allowed estimates (e.g., Throop & Esposito 1998) of the potential hazards to Cassini; these rings are primarily populated by micron-sized grains that will not harm the spacecraft or its instruments.

Saturn's ring-plane crossings, which occurred in late 1995, have been analyzed (the earliest, but still most comprehensive, presentation is by Nicholson et al. 1996). The ring's edge-on thickness is measured as 1.2 to 1.5 km, but seems to be dominated by the slightly tilted F ring, which masks the main ring; this small inclination of the F ring to the main ring's plane may also explain why the exact times of the crossing at east and west ansae differ. Most small moons that skim just beyond the main rings were discovered during previous ring-plane crossings (when the main rings' glare is much reduced) or by Voyager; they were next visible during the 1995 crossings fifteen years later. The orbits of both of the F-ring's shepherd satellites appear to have changed from those by Voyager; models are under study to test whether these perturbations result from interactions with known/unknown satellites or from recoil off the ring wakes. Many "objects" that were initially believed to be satellite discoveries are now interpreted as due to transient arcs or clumps of material in the F ring's vicinity.

Numerical simulations by French and US (Arizona) scientists have been reasonably successful in demonstrating that the Neptunian ring-arcs can be stabely populated. However, HST and ground-based (Sicardy et al. 1999) measurements of the precise locations of the arcs call into question whether the generally accepted resonant solution works.

References

Burns, J. A., Showalter, M. R., Hamilton, D. P., Nicholson, P. D., de Pater, I., Ockert-Bell, M., & Thomas, P. C. 1999, Science, 284, 1146-1150

Cuzzi, J. N., & Estrada, P. R. 1998, Icarus, 132, 1-35

Grun, E., Kruger, H., Graps, A., Hamilton, D. P. et al. 1998, JGR, 103, 20,011-20,022

Krivov, A. V., & Hamilton, D. P. 1997, Icarus, 128, 335-353

Nicholson, P. D., Showalter, M. R., Dones, L., French, R. G., Larson, S. M., Lissauer, J. J., McGhee, C. A., Seitzer, P., Sicardy, B., & Danielson, G. E. 1996, Science, 272, 509-515

Ockert-Bell, M. E., Burns, J. A., Daubar, I. J., Thomas, P. C., Veverka, J., Belton, M. J. S., & Klaasen, K. P. 1999, Icarus, 138, 188-213

de Pater, I., Showalter, M. R., Burns, J. A., Nicholson, P. D., Liu, M. C., Hamilton, D. P., & Graham, J. R. 1999, Icarus, 138, 214-223

Sicardy, B., Roddier, F., Roddier, C., Perozzi, E., Graves, J. E., Guyon, O., & Northcott, M. J. 1999, Nature, 400, 731-733

Throop, H. B., & Esposito, L. W. 1998, Icarus, 131, 152-166

9. JUPITER ICY GALILEAN SATELLITES: SURFACE COMPOSITION

(Contributed by Thomas B. McCord, Hawaii Institute of Geophysics and Planetology, Honolulu, USA)

Surface compositional information for the Galilean satellites was provided first by groundbased telescope spectroscopic observations. Subsequently, orbital telescopes (IUE, HST, ISO) and spacecraft (Voyager, Galileo) have provided broader wavelength coverage and/or higher spatial resolution data. The surfaces of the outer three Galilean Satellites – Europa, Ganymede and Callisto – are dominated by water ice (Kuiper 1957; Harris 1961). Moroz (1965) Johnson and McCord (1971). Pilcher et al. (1972) Fink et al. (1973; 1975). Non-ice materials, including unidentified hydrated materials, were reported as well. The amounts and proportions of ice to non-ice materials has been somewhat difficult to determine, with grain-size, layering and multiscattering effects complicating the interpretations (e.g., Clark 1980, 1981; Clark & McCord 1980). The consensus was that Callisto's surface is covered at 60-80% by non-icy components, with Ganymede and then Europa being increasingly icier. Photometric differences between trailing and leading sides of the satellites were noted.

Voyager multispectral images show that a UV-absorbing material of exogenic origin, such as a form of sulfur, contaminates the trailing side of Europa, producing "stains" overlaying the endogenic geologic albedo patterns (Johnson et al. 1983; McEwen 1986; Nelson et al. 1986; Nelson et al. 1987; Johnson et al. 1988; Pospieszalska & Johnson 1989). More recently, from groundbased telecscopes and HST, SO_2 or at least some form of S - O bond was reported on the trailing side of Europa (Lane et al. 1981; Noll et al. 1995) and on the leading side of Callisto (Noll et al. 1997). Ozone (Noll et al. 1996) and molecular oxygen (Spencer et al. 1995) were also reported on the trailing side of Ganymede. Except perhaps for SO_2 on Callisto, these species are thought to be induced by radiation chemistry. The Galileo Mission and in particular the Near Infrared Mapping Spectrometer (NIMS) (e.g., Carlson et al. 1996) produced a wealth of new spectroscopic and image data revealing much new information about the surface composition of the Galilean Satellites. The first spectra analyzed were for a polar region on Europa, which exhibited mostly water-frost features (Carlson et al. 1996). Later NIMS data revealed distorted water spectral features for areas

on the trailing side of Europa similar to those seen in telescopic observations. These were interpreted to indicate hydrated minerals of some sort (Carlson et al. 1997a,b ; Granahan et al. 1997). McCord et al. (1998a; 1999) suggested hydrated sulfates and carbonates to explain the distorted water absorptions found in darker regions of the trailing side, perhaps confirming earlier model predictions (Fanale et al. 1997; Kargel 1991). However, Dalton and Clark (1998a,b) suggested that long optical paths through ice might be the explanation. McCord et al. were unable to confirm this using radiative transport models. Recently, Carlson et al. (1999) suggested that sulfuric acid is also present, along with its radiolysis products and that such an assemblage can account for many characteristics of the IR and visible spectra. The hydrated minerals are concentrated at the lineaments and in chaotic terrain, which are tectonically disrupted areas on the trailing side. Since the spectrum of the hydrates on Europa is nearly the same everywhere so far studied, the composition may be nearly uniform. This suggests similar sources and processes over at least a near-hemispheric scale. Therefore, if the hydrate is a salt or mixture of salts, then a circulating subsurface ocean containing dissolved salts could be the source. Five new absorption features were reported from the NIMS data at 3.4, 3.88, 4.05, 4.25 and 4.57 μm for Callisto and Ganymede and some seem to exist for Europa as well (McCord et al. 1997; 1998b). Suggested candidate spectrally active groups, perhaps within larger molecules, producing the five absorptions include C-H, S-H, SO_2, CO_2, and C≡N, respectively. Organic materials like tholins are candidates for the 4.57- and 3.4-μm features. Carlson (1999) reported detection of a CO_2 exosphere over Callisto, helping confirm the surface CO_2 interpretation. The four absorption bands strong enough to be mapped on Callisto and Ganymede are each spatially distributed in different ways, indicating different materials are responsible for each absorption. The spatial distributions are correlated at the local level in complex ways with surface features and in some cases show global patterns. Elevated CO_2 is associated with younger, ice-rich impact features over the entire surface of Callisto, but is not necessarily in the ice. There is also a hemispherical asymmetry, with CO_2 concentrated on the trailing hemisphere, which may be an effect of Jupiter's co-rotating magnetic field. Ganymede does not exhibit these patterns, but the generally equatorially distributed CO_2 is most strongly associated with the more ice-free materials.

References

Carlson R., Smythe, W., Baines, K., Barbanis, E., Becker, K., Burns, R., Calcutt, S., Calvin, W., Clark, R., Danielson, G., Davies, A., Drossart, P., Encrenaz, T., Fanale, F., Granahan, J., Hansen, G., Herrera, P., Hibbitts, C., Hui, J.,Irwin, P., Johnson, T., Kamp, L., Kieffer, H., Leader, F., Lellouch, E., Lopes-Gautier, R., Matson, D., McCord, T., Mehlman, R., Ocampo, A., Orton, G., Roos-Serote, M., Segura, M., Shirley, J., Soderblom, L., Stevenson, A., Taylor, F., Torson, J., Weir, A. & Weissman, P. 1996, Science, 274, 385-388, 1996.

Carlson, R. W. and the NIMS Team 1997a, in: Remote Sensing of Planetary Ices: Earth and Other Solid Bodies (Flagstaff, Arizona, June 11-13)

Carlson, R. W. 1997b, in : Annual Mtg. Geological Society of American (Salt Lake City, October 22)

Carlson, R. W. 1999, Science, 283, 820-821

Carlson, R. W., Johnson, R. E. & Anderson, M. S. 1999, Science, in press

Clark, R. N. 1980, Icarus, 44, 388-409

Clark, R. N. 1981, J. Geophys. Res., 86, 3074 3086

Clark, R. N. & McCord, T. B. 1980, Icarus, 41, 323-339

Dalton, J. B. & Clark, R. N. 1998a, Bull. Am. Astron. Soc., 30, 1081

Dalton, J. B. & Clark, R. N. 1998b, EOS, 79, F541

Fanale, F. P., Johnson, T. V. & Matson, D. L. 1977, in: Planetary Satellites, ed. J. A. Burns (University of Arizona Press: Tucson) 379-406

Fink, U., Dekkers, N. H. & Larson, H. P. 1973, Astrophys. J., 179, L155-L159

Fink, U. & Larson, H. P. 1975, Icarus, 24, 411

Granahan, J. C., Fanale, F. P., McCord, T. B., Hansen, G. B., Carlson, R. W., Kamp, L., Matson, D., Ocampo, A., Smythe, W., Hendrix, A. R., Barth, C. A., Leader, F., Melhman, R., Greeley, R., Sullivan, R., Clark, B. E., Helfenstein, P., Veverka, J., Geissler, P., Belton, M. J. S., Becker, K., Becker, T. & Cook, D. 1997, Bull. Am. Astron. Soc., 29, 982

Harris, D. L. 1961, in: Planets and Satellites, ed. G. P. Kuiper & B. M. Middlehurst (Univ. of Chicago Press, Chicago) 305

Johnson, T. V. and McCord, T. B. 1971, Astrophys. J., 169, 589-594

Johnson, T. V., Soderblom, L. A., Mosher, J. A., Danielson, G. E., Cook, A. F. & Kupperman, P. 1983, J. Geophys. Res., 88, 5789-5805

Johnson, R. E., Nelson, M. L., McCord, T. B. & Gradie, J. C. 1988, Icarus, 75, 423-436

Kargel, J. S. 1991, Icarus, 94, 368-390

Kuiper, G. P. 1957, Astron. J. 62, 245

Lane, A. L., Nelson, R. M. & Matson, D. L. 1981, Nature, 292, 38-39

McCord, T. B., Carlson, R. W., Smythe, W. D., Hansen, G. B., Clark, R. N., Hibbitts, C. A., Fanale, F. P., Granahan, J. C., Segura, M., Matson, D. L., Johnson, T. V., Martin, P. D. and the NIMS Team, 1997, Science, 278, 271-275

McCord T. B., Hansen, G. B., Fanale, F. P., Carlson, R. W., Matson, D. L., Johnson, T. V., Smythe, W. D., Crowley, J. K., Martin, P. D., Ocampo, A., Hibbitts, C. A., Granahan, J. C. and the NIMS team 1998a, Science, 280, 1242-1245

McCord, T. B., Hansen, G. B., Clark, R. N., Martin, P. D., Hibbitts, C. A., Fanale, F. P., Granahan, J. C., Segura, M., Matson, D. L., Johnson, T. V., Carlson, R. W., Smythe, W. D., Danielson, G. E. and the NIMS Team, 1998b, J. Geophys. Res., 103, 8603-8626

McCord, T. B., Hansen, G. B., Matson, D. L., Johnson, T. V., Crowley, J. K., Fanale, F. P., Carlson, R. W., Smythe, W. D., Martin, P. D., Hibbitts, C. A., Granahan, J. C., Ocampo, A. and the NIMS team, 1999, J. Geophys. Res., 104, 11827-11851

McEwen, A. S. 1986, Nature, 321, 49-51

Moroz, V. I. 1965, Astron. Z., 42, 1287-1295, (in Russian), Trans. Soviet. Astron. A.J., 9, 999-1006

Nelson, M. L., McCord, T. B., Clark, R. N., Johnson, T. V., Matson, D. L., Mosher, J. A. & Soderblom, L. A. 1986, Icarus, 65, 129-151

Nelson, R. M., Lane, A. L., Matson, D. L., Veeder, G. J., Buratti, B. J. & Tedesco, E. F. 1987, Icarus, 72, 358-380

Noll, K. S., Weaver, H. A. & Gonnella, A.M. 1995, J. Geophys. Res., 100, 19,057-19,059

Noll, K. S., Johnson, R. E., Lane, A. L. Domingue, D. L. Weaver, H. A. 1996, Science, 273, 341-343

Noll, K. S., Johnson, R. E., McGrath, M. A. & Caldwell, J. J. 1997, Geophys. Res. Lett., 24, 1139-1142

Pilcher, C. B., Ridgway, S. T. & McCord, T. B. 1972, Science, 178, 1087-1089

Pospieszalska, M. K. & Johnson, R. E. 1989, Icarus, 78, 1-13

Spencer, J. R., Calvin, W. M. & Person, M. .J. 1995, J. Geophys. Res., 100, 19,049-19,056

10. GALILEAN SATELLITES GEOLOGY

(Contributed by Robert T. Pappalardo, Brown University, Providence, USA)

In the past three years, major advances in the understanding of icy outer planet satellites have come from analysis of Jupiter's Galilean satellites - Callisto, Ganymede, Europa, and Io - based on data obtained by the Galileo spacecraft. The geological processes of volcanism, tectonism, cratering, and mass wasting are each significant, with their surface manifestations and relative significance varying among the satellites. With the curious exception of Callisto, the Galilean satellites are found to be highly differentiated. The icy Galilean satellites may have internal liquid water layers, and Io an internal magma ocean.

Doppler gravity data has been used to infer the axial moment of inertia and thus the interior structure of each of the Galilean satellites. Along with bulk density and likely material components, the axial moment of inertia C/MR^2 is used to constrain the internal structure of the satellites. Io is inferred to have a metallic core approximately half the satellite radius, overlain by rocky material. Europa most probably has a metallic core beneath a silicate mantle topped by an H_2O (ice and perhaps water) layer ~80 to 150 km (nominally 100 km) thick. Ganymede's very low C/MR^2 (0.3105 ± 0.0028) indicates an outer ice layer ~800 km thick above a silicate mantle and iron-rich core; in order to explain the satellite's intrinsic magnetic field, the metallic core is probably partially molten. Callisto has a relatively high C/MR^2 (0.359 ± 0.005); this value implies the absence of an iron core, but instead implies differentiation into a rocky core and an ice-rich upper crust.

Voyager images showed that Callisto is heavily cratered at the global scale. A surprise of the Galileo mission is the dearth of small (kilometers and smaller) craters on Callisto. Much of the satellite's surface is blanketed by smooth dark material. This may be a sublimation-derived lag deposit overlying an icy substrate, redistributed by impacts and mass wasting. Evidence for mass wasting includes landslide-like lobes of dark material which have moved downslope into crater floors. Loss of CO_2 "bedice" offers a viable mechanism for creation of a Callistoan surface lag. High-standing knobs and crater rims are bright, suggesting thermal segregation of the surface into ice-rich and ice-poor regions.

Aside from tectonic features (concentric graben and scarps) associated with its large impact structures, the satellite has apparently had an uneventful tectonic and volcanic history, concordant with its only partially differentiated interior. However, Galileo magnetometer data shows strong evidence for an induced magnetic field at Callisto, implying a highly conductive interior. Surprisingly this suggests the presence of an internal briny ocean that has persisted to the present day beneath Callisto's barren surface.

Ganymede's ancient dark terrain is extremely heterogeneous in albedo at small scales and has been modified by tectonism, ejecta blanketing, and mass wasting, along with concentration of a thin dark surficial lag. The satellite's bright grooved terrain is pervasively deformed at multiple scales and is locally highly strained, consistent with extensional necking and local tilt-block normal faulting of its ice-rich lithosphere. The high extensional strain indicated by Galileo images, along with new laboratory data on the rheology of ice, suggests that extensional boudinage is a viable model for forming grooved terrain. The role of icy volcanism in grooved terrain remains uncertain, as no definitive cryovolcanic features have been observed, and normal faulting alone apparently has created some groove lanes. Galileo images suggest revisions to previously inferred stratigraphy of grooved terrain, in that simple cross-cutting and truncation of older groove sets by newer ones can explain the observed stratigraphic relationships. Groove lanes can have consistent orientations over great distances, implying that global stresses may have influenced their formation. Magnetometer data demonstrate the presence of an intrinsic magnetic field at Ganymede (implying a partially molted metallic core). High latitude field lines are open to jovian plasma; charged particles which impinge onto ice at high latitudes may produce the satellite's bright polar caps.

Sparse craters suggest that Europa's icy surface is young and potentially geologically active today. Dynamical modeling of potential impactors (principally Jupiter family comets)

suggests a surface age of 50 million years. This is consistent with age estimates based on estimated surface sputtering rates, and based on the lack of any detectable surface changes since the Voyager era. Europa's bright plains are criss-crossed by narrow troughs and enigmatic doublet ridges (paired ridges separated by a medial trough). Ridge origin is uncertain, but plausible ridge models suggest an origin involving intrusion and/or extrusion of liquid water and/or warm ice. A morphological (and hence inferred evolutionary) sequence is observed from isolated troughs to doublet ridges to wider and more complex ridge morphologies. "Triple bands" are ridges with ruddy diffuse margins; these dark margins may have formed through thermal alteration, cryovolcanism, and/or mass wasting. Wider pull-apart bands have formed by complete separation and spreading of the icy lithosphere, in a manner which may be broadly analogous to terrestrial sea-floor spreading.

Cross-cutting relationships indicate that Europa's dark bands brighten and fade with age. The sequence of ridge formation (inferred based on cross-cutting and color/brightness relationships) suggests that preferred ridge orientation has changed systematically over time in a way consistent with nonsynchronous rotation of the satellite's surface. This implies that the icy surface has been decoupled from the silicate interior, perhaps by an intervening liquid layer. Comparison of Voyager and Galileo images limits the current nonsynchronous rotation period to >12,000 years. The global pattern of Europa's lineaments implies that nonsynchronous stresses and orbital flexing ("diurnal") stresses have combined to fracture Europa's icy shell. Diurnal stressing may explain Europa's extremely enigmatic cycloid ridge and fracture patterns, and may drive strike-slip faulting along ridges and bands. Significant tidal amplitudes are necessary to produce significant diurnal stressing, arguing for a subsurface liquid layer.

Relatively dark and red "mottled terrain" consists of pits, domes, dark spots, patches of smooth plains-forming material, and regions of chaos terrain. Chaos terrain is characterized by fragmented blocks of the preexisting ridged plains which have translated by as much as a few kilometers from their original positions in a dark hummocky matrix. Mottled terrain landforms suggest surface disruption along with localized partial melting. Their formation has been interpreted related to solid-state convection of the warm icy subsurface. If so, "hot" ice diapirs could be triggering partial melting of a salty ice shell. Alternatively, these features have been interpreted as indicative of complete melt-through of Europa's icy shell from an ocean below. Both models imply high heat flow, larger than predicted by simple models of tidal and radiogenic heating. Interestingly, measurements from the Galileo Photopolarimeter-Radiometer instrument shows unusually high nighttime temperatures which might indicate high endogenic heat flow. Magnetometer data are suggestive of an induced magnetic field, or possibly a dipole field with an unusually steep tilt. An induced field would suggest interior briny liquid water. Thermal models predict that tidal heating might maintain a liquid ocean within Europa today, and this intriguing hypothesis is consistent with (but unproven by) Galileo results. A Europa Orbiter mission is in the planning stages and would be able to provide definitive geophysical tests for a Europan ocean.

Tidal heating makes Io the Solar System's most volcanically active body. From a distance Galileo has monitored eruptions and surface changes on this dynamic satellite at ultraviolet through infra-red wavelengths. Imaging has documented significant surface changes from the Voyager era and within the Galileo era. For example the Prometheus plume, active during the Voyager era, has also been active during the entire Galileo tour, but the plume location has shifted by some 70 km from the Voyager location. Many new volcanic centers have been identified, including Pillan, unknown until Galileo's tenth orbit. Plume deposits are commonly red in color and apparently fade with age, suggesting the presence and breakdown of sulfur allotropes. The collective population of Io's active and inactive volcanic centers is found to be randomly distributed.

Galileo observations in eclipse show visible and infra-red emissions from Io, including airglow. Clusters of hot spots are observed in Io's sub- and anti-jovian regions. Based on visible and infra-red intensities, black-body curves have been fit to hot spot temperature

estimates, indicating that some of Io's vents erupt lavas with temperatures greater than 1600 K, hotter than any on current-day Earth. This requires silicate (rather than sulfur) volcanism, probably ultramafic silicates. This interpretation is consistent with multispectral imaging data which show an absorption consistent with magnesium-rich pyroxene. Such high eruption temperatures suggest that Io may posses a global magma ocean. Close Galileo encounters of Io, which will include very high resolution imaging, are planned for the final months of 1999.

The Cassini spacecraft was launched successfully in October 1997 toward a 2004 arrival at Saturn. Its multiple fly-bys of the saturnian satellites will provide fruitful information on their geology, allowing for comparison to the geology of the Galilean moons.

11. JUPITER MAGNETIC FIELDS AND PARTICLES

(Contributed by Margaret G. Kivelson, University of California, Los Angeles, USA)

The last triennium has witnessed an explosion of new results on Jupiter and its satellites based on the in situ data of the Galileo Orbiter (capture orbit achieved in December 1995) and the remarkable images provided by Hubble Space Telescope instruments. The images reveal an aurora generally narrow in latitude and rather quiescent near dawn, becoming broader and more dynamic in the afternoon quadrant where it reveals distinct structure that rotates with Jupiter. The brightest portion of the aurora is in the dawn sector. Towards dusk, the aurora fills large parts of the polar cap. On the night side of the planet, it continues as a narrow zone of emission at lower latitudes than on the day side. The ultraviolet images show not only the aurora but also localized features linked along the Jovian magnetic field to the moons Io, Europa, and Ganymede. The bright spot at the foot of Ganymede's magnetic flux tube (footprint) appears at lower latitude than the aurora, thus ruling out unambiguously the possibility that the aurora links to Io's orbit. There is now no doubt that the dominant auroral zone maps to regions well beyond 15 R_J (jovian radii). The location of the Io footprint (observed also in infrared measurements from the ground) has been traced as a function of Jupiter longitude, providing constraints on the higher order (than dipole) moments of the Jovian magnetic field. A faint trail of luminosity leads Io's auroral footprint over more than 100 degrees of longitude, showing that the plasma in Io's orbit is strongly coupled to Jupiter's ionosphere.

It was already apparent from earlier spacecraft measurements (Pioneer 10 and 11, Voyager 1 and 2, and Ulysses) that Jupiter's magnetospheric magnetic field is greatly distended by an extensive equatorial current sheet present through much of the morning hemisphere. However, the flyby orbits of these earlier spacecraft precluded any investigation of the local time structure of the current sheet or its dynamics. In the past three years, Galileo's orbit has swept out a large part of the nightside equatorial magnetotail. Although analysis is still incomplete, there is clear evidence of strong local time variation. The field twists out of meridian planes more in the midnight to dawn sector than in the pre-midnight sector. The implied pattern of plasma transport has not yet been fully interpreted. That the tail experiences dynamic changes, occasionally apparently periodic with a period of a few days, is evident from the occurrence of bursty flows of energetic particles associated with variations of the intensity of hectometric radiation and fluctuations in the magnetic field orientation. It is not yet clear whether the observations can be explained purely in terms of internal drivers (plasma added to the system near Io's orbit tearing free of the confining magnetic field as it rotates into the magnetotail) or whether changing solar wind conditions play an important role. Near Io's orbit, Galileo detected small-scale, nearly empty flux tubes moving rapidly through higher density flux tubes, implying a pattern of transport by interchange quite different from that anticipated in previous theoretical analysis.

Perhaps the most surprising observations at Jupiter relate to the plasma interactions near the Galilean moons and to the magnetic properties of these planetary size objects. The moons, orbiting Jupiter at Keplerian velocities, are embedded in the heavy ion plasma of the Io plasma torus, which overtakes them from their trailing sides. Near Io, known to be the source of much of the magnetospheric plasma, the plasma density was expected

to increase. Galileo's pass in December 1995 revealed that the plasma density is even higher than expected. The density increased by almost an order of magnitude relative to the background on the leading edge of Io (thus downstream in the plasma flow), with strong field-aligned fluxes of electrons as energetic as ~100 keV present near the center of the wake. It is likely that these electron beams arise through a process that creates the footprint aurora, but details have not yet been worked out. A large depression in the magnetic field was observed near closest approach to Io. The magnitude of the depression suggests that Io has an internal magnetic moment, but alternative explanations have been proffered and the resolution must await data from additional passes near Io anticipated before the end of 1999. For Ganymede, the evidence of a large internal dipole moment is unambiguous. The field is large enough to exclude the ambient Jovian magnetic field from a volume surrounding the moon, thus creating the first known magnetosphere of a moon. Dynamo theorists are challenged by the need to account for the persistence of a large magnetic moment in a body that should long ago have cooled to temperatures low enough to make a dynamo impossible.

The moons Europa and Callisto have icy surfaces. Remarkably, in several Galileo passes magnetic perturbations consistent with generation by inductively driven near-surface currents were observed. A plausible interpretation is that the induced currents flow in salty near-surface oceans. The interpretation suggests unexpectedly complex internal structure. Additional passes have been planned to test the interpretation in the next year.

Many of the findings summarized above are discussed fully in (Bagenal 1998) and articles that follow.

References

Bagenal, F. 1998, J. Geophys. Res., 103, 19, 841-2

12. PLUTO, CHARON, AND TRITON

(Contributed by Dale P. Cruikshank, NASA Ames Research Center, USA, and Catherine de Bergh, Observatoire de Paris, France)

Physical studies of Pluto and Charon have continued by the methods of near-infrared spectroscopy, both from ground-based observatories (Douté et al. 1999; Geballe et al. 1999) and with the Hubble Space Telescope (Dumas et al. 1998). It has become possible to separate the spectral contributions of the planet and its satellite, although they are only 0.9 arc-sec apart, by the use of adaptive optics and other seeing compensation techniques (at ground-based telescopes), and by the high spatial resolution afforded by the HST. Pluto's inventory of detected molecules includes solid N_2, CH_4, CO, and H_2O. The CO and some of the CH_4 are dissolved in solid N_2, while some of the CH_4 appears in a pure state in spatially isolated surface patches (Douté et al. 1999). Although theoretical models (Lara et al. 1997; Krasnopolsky & Cruikshank 1999) predict the presence of numerous other hydrocarbons, HC_3N and HCN, none of these molecules has yet been detected. Important laboratory studies of ices of relevance to Pluto and other outer Solar System bodies were published (Quirico & Schmitt 1997a,b ; Grundy & Schmitt 1998).

Whereas previous work (Buie et al. 1987) indicated that Charon's hemisphere visible from Earth at superior conjunction is largely covered by water ice, the more recent work (Geballe et al. 1999) shows that water ice is the dominant surface component on th e remaining parts of the surface, seen at northern and southern orbital elongations. With knowledge of the uniform distribution of water ice on Charon, it now appears that water ice previously detected on Pluto itself is confined to a relatively narrow range of longitude near the region of the planet visible at the minimum in its rotational lightcurve (Cruikshank et al. 1999a).

A major study of the surface composition of Triton was published (Quirico et al. 1999), in which the distribution of the detected components (N_2, CH_4, CO, CO_2, H_2O) was

detailed. The detection and distribution of H_2O was further elaborated in a related paper (Cruikshank et al. 1999b).

Observations of stellar occultations by Triton in 1995 (Olkin et al. 1997) and 1997 (Elliot et al. 1998; Sicardy et al. 1998) indicate that the atmospheric surface pressure on the satellite has increased significantly since the 1989 Voyager detection of the largely N_2 atmosphere. A conservative estimate of the rate of temperature and surface-pressure increase during this period implies that the atmospheric mass is doubling every 10 years, probably as a result of seasonal changes. Observations of episodic changes in the color of Triton in the 0.4-0.95 μm spectral range were also reported (Buratti et al. 1999).

References

Buie, M. W., Cruikshank, D. P., Lebofsky, L. A., & Tedesco, E. F. 1987, Nature, 329, 522-523

Buratti, B. J., Hicks, M. D., & Newburn, Jr., R. L. 1999, Nature, 397, 219.

Cruikshank, D. P., Schmitt, B., Owen, T. C., Douté, S., Geballe, T. R., de Bergh, C., Dalle Ore, C. M., & Roush, T. L. 1999a, (in preparation).

Cruikshank, D. P., Roush, T. L., Owen, T. C., Schmitt, B., Quirico, E., Geballe, T. R., de Bergh, C., Bartholomew, M. J., Dalle Ore, C. M., Douté, S., & Meier, R. 1999b, Icarus (submitted)

Douté, S., Schmitt, B., Quirico, E., Owen, T. C., Cruikshank, D. P., de Bergh, C., Geballe, T. R., & Roush, T. L. 1999, Icarus (in press)

Dumas, C., Terrile, R. J., Burgasser, A., Brown, R., Rieke, M., Schneider, G., Thompson, R., & Koerner, D. 1998, Bull. Am. Astron. Soc., 30, 1108 (abstract)

Elliot, J. L. et al. 1998, Nature, 393, 765-767

Geballe, T. R., Cruikshank, D. P., Dalle Ore, C. M., & Owen, T. C. 1999, Icarus (submitted)

Grundy, W., & Schmitt, B. 1998, J. Geophys. Res. 103, 25,809-25,822

Krasnopolsky, V. A., & Cruikshank, D. P. 1999, J. Geophys. Res. (in press)

Lara, L. M., Ip, W. -H., & Rodrigo, R. 1997, Icarus, 130, 16-35

Olkin, C. B. et al. 1997, Icarus, 129, 178-201

Quirico, E., & Schmitt, B. 1997a, Icarus, 127, 354-378

Quirico, E., & Schmitt, B. 1997b, Icarus, 128, 181-188

Quirico, E., Douté, S., Schmitt, B., de Bergh, C., Cruikshank, D. P., Owen, T. C., Geballe, T. R., & Roush, T. L. 1999, Icarus, 139, 159-178

Sicardy, B. et al. 1998, Bull. Am. Astron. Soc., 30, 1107 (abstract)

13. TITAN

(Contributed by Athéna Coustenis, Observatoire de Paris, France)

With the Cassini/Huygens mission to Titan and the Saturnian system well underway, we are now 5 years from unravelling the wonderful mysteries of Saturn's largest satellite and from testing the numerous models which exist on its atmosphere and surface. Regarding the atmosphere, most models until now were based on observations performed by the Voyager 1 spacecraft in 1980. These determined the composition and temperature structure of Titan's atmosphere at the time of the Voyager encounter at various locations over its disk. The surface of the satellite, however, remained an unknown after this flyby, because the satellite is enshrouded in a thick cloud mantle. Some models, based on Voyager data, predict methane supersaturation in the troposphere of Titan (e.g. Samuelson et al. 1997). In the past few years, though, numerous breakthroughs have been achieved in Titan science, thanks to both ground-based and space observatories. Thus, the pathway for the Cassini arrival in 2004 is well prepared (for a summary of current pre-Cassini Titan knowledge, see for instance Coustenis & Taylor, 1999).

In 1997, the Infrared Space Observatory (ISO) contributed significant observations of Titan in the 7-45 μm region, probing the satellite's stratosphere as a disk-average. These measurements come almost exactly two Titan seasons after the Voyager encounter and afford higher spectral resolution than the Voyager spectrometer. Thus, the chemical composition of the satellite as a disk average is precisely determined and a temperature profile is established in the stratosphere. A new estimate of the D/H ratio from the CH_3D band at 8.6 μm indicates a nominal value of about 10^{-4}, compatible with both the Voyager measurement and ground-based observations, a ratio significantly lower than that observed in comets, suggestive of a non-cometary origin of Titan's atmosphere. But the most important contribution to Titan science of the ISO Short Wavelength Spectrometer is the first detection of two water vapor emission lines at 39.7 and 43.9 μm, at the 8-σ level, after about 3 hours of integration time and careful analysis (Coustenis et al. 1998). The retrieved abundance is around 10^{-8} at the 400-km level. The inferred water influx on Titan is quite large with respect to the one on Saturn (ratio in the range of 1 to 6).

Considerable progress has also been made in the past few years on the study of Titan's lower atmosphere and surface through radio experiments, but also, mainly, by exploring the near-infrared range by imaging and spectroscopy. The 1-5 μm spectral region on Titan has offered the opportunity to probe the lower atmosphere and surface of the satellite through specific low methane absorption atmospheric "windows". Lightcurves of Titan's surface have established its inhomogeneity, indicating that the leading hemisphere is significantly brighter than the trailing hemisphere. Also, spectra from September 1995 (1.4-3.2μm) show unexpectedly high albedos in three of Titan's atmospheric windows. Griffith et al. (1998) interpret the high albedos as evidence of methane clouds in the troposphere. The surface albedo spectrum derived from near-IR spectroscopy is compatible with the presence of water ice as the major constituent on the ground, mixed with tholin deposits, and also possibly a rocky component. More observations are however required before the nature of Titan's surface is established.

Imaging of Titan's surface at different orbital phases has been achieved by the Hubble Space Telescope (Smith et al. 1996) and by using adaptive optics systems on the ground (ESO/Chile, PUEO/CFHT, Keck). These images show a large bright region in images taken at 0.94, 1.29, 1.6 and 2 μm, extending over 60 degrees of longitude and 30 degrees of latitude near Titan's equator, on the leading side. Also, bright zones were found at higher latitudes on the trailing hemisphere and probably all over the disk (Combes et al. 1997), and could be compatible with the presence of polar caps. The presence of the bright equatorial region on the leading hemisphere is in agreement with the spectroscopic observations. The Huygens probe will land on Titan's surface in 2004.

References

Combes, M. et al. 1997, Icarus, 129, 482-497

Coustenis A. et al. 1998, A&A, 336, L85-L89

Coustenis, A. & Taylor, F. 1999, Titan: the Earth-Like Moon, World Scientific Publ., Singapore

Griffith, C. et al. 1998, Nature, 395, 575-578

Samuelson, R. et al. 1997, Plan. Space Sci., 45, 959-980

Smith, P. et al. 1996, Icarus, 119, 336-349

14. IRREGULAR SATELLITES OF URANUS

(Contributed by B. Gladman, Observatoire de Nice, France)

In September 1997, the first two irregular satellites of Uranus, provisionally designated S/1997 U1 and S/1997 U2, were discovered by B. Gladman, P. Nicholson, J. A. Burns, and J. Kavelaars (IAU Circ. 6704, October 31, 1997). Continued observations of the objects during 1997 eliminated the small possibility that these objects were Centaurs fortuitously passing close to the planet, and their identification in December 1997 on photographic plates taken at CFHT in 1984 by D. Cruikshank provided a 14-year baseline for their orbit computation. With the 1997 data combined with observations in the spring of 1998, fits of the suite of observations made at the Minor Planet Center and independently at JPL, give accurate elements for both satellites, as listed on IAU Circ. 6869 and 6870. The discoverers have proposed the names Caliban (1997 U1) and Sycorax (1997 U2); these have been accepted by the nomenlature working group, but remain to be approved during the IAU 2000 General Assembly. If the geometric albedos of these two objects are 0.07, the estimated diameters are 120 km for Sycorax and 60 km for Caliban.

The orbits of both Caliban and Sycorax are highly inclined with respect to the orbital plane of Uranus, suggesting that they are captured objects. They are, however, very deep inside the gravity well of the planet, making the common hypothesis of gas drag problematic, since a large amount of binding energy would have to be dissipated in the capture. Color studies performed in 1997 show reddish colors, more similar to trans-neptunian objects than to the inner moons of comparable sizes, thus supporting a capture origin. Additional (as yet unpublished) color data have been acquired by several groups in 1999.

In July, 1999, two additional Uranian satellite candidates were reported in IAU Circ. 7230; these two objects (S/1999 U1 and S/1999 U2) are following the planet across the sky at rates consistent with bound motion, but until a longer arc can be observed, there remains the possibility that they are passing Centaur objects. IAU Circ. 7248 reports additional observations of S/1999 U1 and U2, and detection of a third object, S/1999 U3.

References

Gladman, B., Nicholson, P., Burns, J. A., Kavelaars, J. J., Marsden, B., Williams, G., & Offut, W. 1998, Nature, 392, 897-899

C. de Bergh
President of the Commission

https://doi.org/10.1017/S0251107X00002662 Published online by Cambridge University Press